

# Hadrons in Nuclei

## from High (200 GeV) to Low (1 GeV) energies

K. Gallmeister, M. Kaskulov, U. Mosel\*, P. Mühlich

Institut fuer Theoretische Physik, Universitaet Giessen, Giessen, Germany

November 1, 2018

### Abstract

The study of the interaction of hadrons, produced by elementary probes in a nucleus, with the surrounding nuclear medium can give insight into two important questions. First, at high energies, the production process, the time-scales connected with it and the prehadronic interactions can be studied by using the nuclear radius as a length-scale. We do this here by analyzing data from the EMC and HERMES experiments on nuclear attenuation. Second, at low energies the spectral function, and thus the selfenergy of the produced hadron, can be studied. Specifically, we analyze the CBELSA/TAPS data on  $\omega$  production in nuclei and discuss the importance of understanding in-medium effects both on the primary production cross section and the final state branching ratio. In both of these studies an excellent control of the final state interactions is essential.

## 1 Introduction

The investigation of hadrons in medium is an exciting subject with implications both for hadron physics and the study of the quark-gluon plasma (QGP) state of nuclear matter. The former field of studies is concerned with the interactions of slow-moving hadrons and their selfenergies inside nuclear matter. The latter deals with interactions of fast-moving partons and/or hadrons inside hot and dense nuclear matter; their clarification needs both the properties of the still largely unknown QGP state of nuclear matter and of the interaction of jets with this matter. A study of jet interactions in cold, ordinary nuclear matter of known properties may thus help to disentangle effects of the interaction of jets from those of the medium in which they move. Also, at these high energies the question of production and formation times may be studied by exploiting the final state interactions of the hadrons produced with the surrounding nuclear matter. For this problem the nuclear radius provides a length- and thus also a time-scale during which interactions can take place.

In this paper we briefly describe our studies of the formation times and the interactions during this time. For this purpose we first analyze data both from the EMC ( $\approx 200$  GeV) and from the HERMES collaboration ( $\approx 20$  GeV). In the second part we then move to a discussion at much lower energies (a few 100 MeV) and discuss our present knowledge of in-medium selfenergies of hadrons and their interactions. For details for the former we refer to [1] whereas for the latter we mainly refer to [2].

---

\*mosel@physik.uni-giessen.de

## 2 Prehadronic Interactions

The EMC experiment has yielded data on nuclear attenuation that correspond to average values of  $Q^2 \approx 4 - 12 \text{ GeV}^2$ , corresponding to the two beam energies of 100 GeV and 280 GeV, respectively. However, most of the experiments on nuclear attenuation that have been performed (HERMES, JLAB) work at rather small values of  $Q^2 \approx 1 - 2 \text{ GeV}^2$  so that methods of perturbative QCD are not applicable. We have, therefore, modelled the prehadronic interactions such that the description works at all energy regimes and describes the transition from high to low energies correctly. Our model relies on a factorization of hadron production into the primary interaction process of the lepton with a nucleon, essentially taken to be the free one, followed by an interaction of the produced hadrons with nucleons.

For the first step we use the PYTHIA model that has been proven to be very successful for describing hadron production, also at the low values of  $Q^2$  and  $\nu$  treated in this paper. This model contains not only string fragmentation, but also direct interaction processes such as diffraction and vector meson dominance. In this first step we take nuclear effects such as Fermi motion, Pauli blocking and nuclear shadowing into account [3]. The relevant production and formation times are obtained directly from PYTHIA [4]; for a definition of these times we refer to [1]. In the second step we introduce prehadronic interactions between the production and the formation time and the full hadronic interactions after the hadron has been formed. We do this by means of the semiclassical GiBUU transport code [5] which not only allows for absorption of the newly formed hadrons, but also for elastic and inelastic scattering as well as for side-feeding through coupled channel effects.

The actual time-dependence of the prehadronic interactions presents an interesting problem in QCD. Dokshitzer [6] has pointed out that QCD and quantum mechanics lead to a time-dependence somewhere between linear and quadratic. Kopeliovich et al. [7] have called attention to the fact that the cross sections may even oscillate in time, as a consequence of a quantum mechanical superposition of excited states of the produced hadron. We also note that a linear behavior had been used by Farrar et al. [9] in their study of quasiexclusive processes. In our calculations we work with different time-dependence scenarios, among them a constant, lowered prehadronic cross section, a linearly rising one and a quadratically rising one. In addition, we study a variant of the latter two, where the cross section for leading hadrons, i.e. hadrons that contain quarks of the original target nucleon, starts from a pedestal value  $\sim 1/Q^2$ , thus taking into account possible effects of color transparency (for details see [1]).

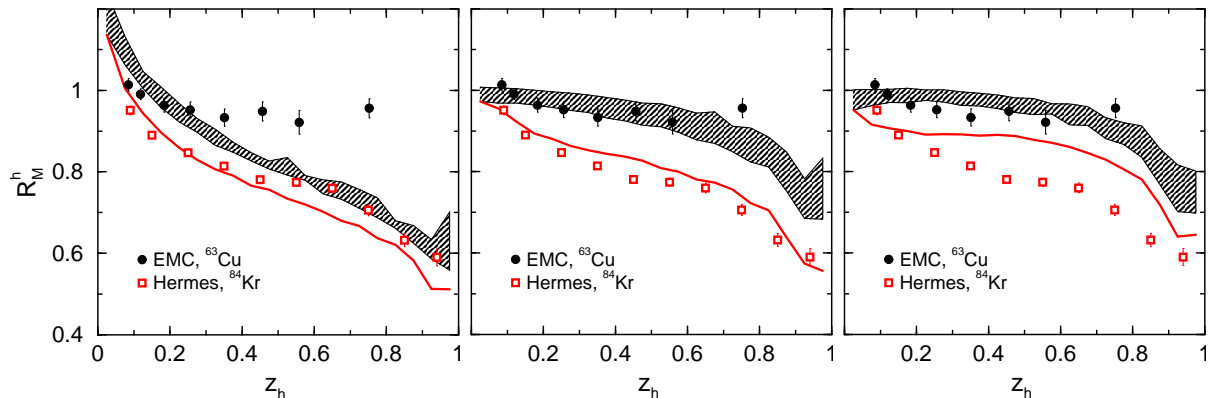


Figure 1: Nuclear modification factor for charged hadrons. Experimental data are shown for HERMES at 27 GeV and for EMC at 100/280 GeV. For the latter the predictions for the upper and lower energy are given by the upper and lower bounds of the shaded band. The cross section scenarios are (from left to right): constant, linear and quadratic increase with time after production.

Fig. 1 shows a comparison of these various model assumptions. It is clearly seen that the assumption of prehadronic cross section reduced to a constant value ( $=0.5$ ) in the leftmost figure leads to a

significantly too large attenuation for the EMC experiment while the HERMES data can be described reasonably well (this should be no surprise since the constant has essentially been fitted to the HERMES data). On the contrary, the quadratic time-dependence gives a good description of the EMC data but underestimates the attenuation significantly for the HERMES data.

This behavior can be understood by looking at the relevant production and formation times depicted in Fig. 2. One sees that the formation times for the EMC experiment at  $z_h \approx 0.8$  approach 30 fm, i.e. values well beyond nuclear radii. This then causes very little attenuation if the prehadronic cross section does not rise fast enough so that the hadron still interacts with the nuclear environment. The

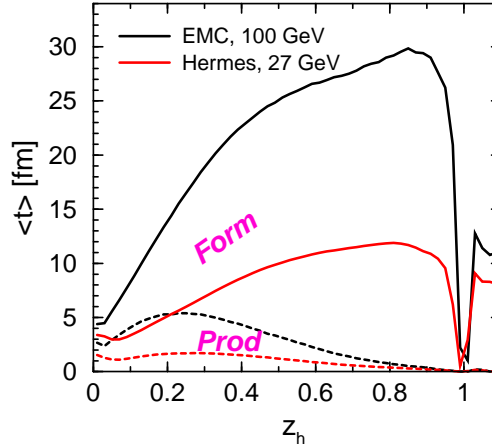


Figure 2: Averaged production (lower 2 curves) and formation times (upper 2 curves) for the EMC (solid) and the HERMES (dashed) experiment. The average contains the times of the leading hadrons as a function of the variable  $z_h$ , defined as the ratio of the hadron's energy to the energy transfer.

middle scenario in Fig. 1 (linear time-dependence) describes the data for all hadrons both for the high-energy EMC experiment and for the lower-energy HERMES experiment very well. This nearly perfect agreement is also seen in Fig. 3 which gives the attenuation  $R$  for pions for the same target nuclei as in Fig. 1 as a function of energy-transfer  $\nu$ , relative energy  $z_h = E_h/\nu$ , momentum transfer  $Q^2$  and the squared transverse momentum  $p_T^2$ . The dependence of  $R$  on all these dynamical variables is described very well. The rise of  $R$  with  $\nu$  is mainly an acceptance effect, as we have shown in [3], whereas the weaker rise of  $R$  with  $Q^2$  reflects the pedestal value  $\sim 1/Q^2$  of the prehadronic cross sections. The  $z_h$ -dependence of  $R$  is – below  $z_h \approx 0.5$  – strongly influenced by final state interactions of fast-moving hadrons that get slowed down by collisions.

The curves in the rightmost column of Fig. 3 show that for the heavier target nuclei the transverse momentum distribution of the nuclear modification factor  $R$  tends towards values  $> 1$  at large  $p_T^2$ . We investigate this phenomenon in more detail with the help of the results obtained for the lower JLAB energy of 5 GeV, shown in Fig. 4. Here it is seen that the  $p_T$  distributions reach farther out for heavier nuclei than for a light  $D$  target. This is a consequence of hadronic rescattering and obviously leads to the observation that  $R > 1$  at these high  $p_T$ . That the  $p_T$  distributions reach out farthest for intermediate  $z_h$  values is due to simple kinematic constraints. Prehadronic interactions have little effect on this observable as can be seen by comparing the upper two curves (with and without prehadronic interactions) with each other. It can also be seen that the results for  $Pb$  and for  $D$  agree with each other for low to moderate transverse momenta. Only at the highest transverse momenta a nuclear effect appears. As a consequence, the expectation values  $\langle p_T^2 \rangle$  are hardly affected by rescattering and are thus not a good indicator for any rescattering (be it hadronic or prehadronic) effects.

With this method we have also calculated the recently measured transmission of large  $z$  pions moving in forward direction through a nucleus [10]. Again a very good agreement of theory and experiment is

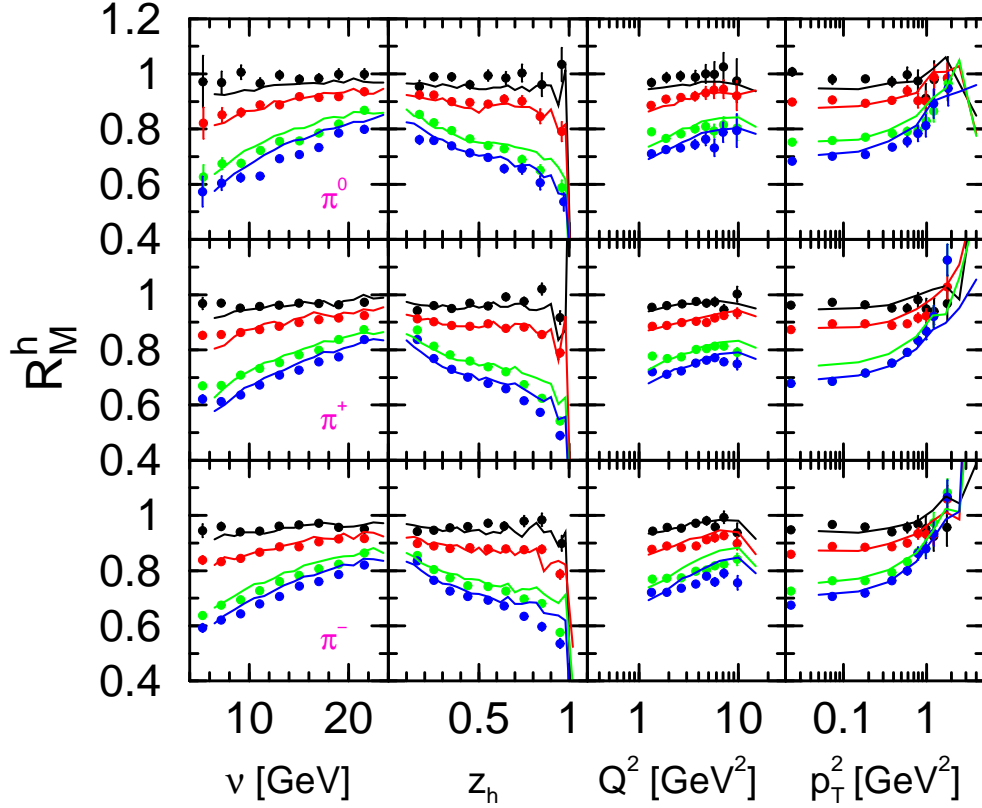


Figure 3: Attenuation of pions in comparison with results of the HERMES experiment. Target nuclei are  ${}^4\text{He}$ ,  ${}^{20}\text{Ne}$ ,  ${}^{84}\text{Kr}$  and  ${}^{131}\text{Xe}$  (curves from top to bottom). The calculations have been done with the linear increase of the prehadronic cross sections and a pedestal value for the leading hadrons  $\sim 1/Q^2$ . Experimental acceptance limitations are taken into account. Data are from [8].

reached [11].

Summarizing this section we can say that our event simulation gives a very good description of nuclear attenuation data over a wide (5 GeV - 200 GeV) energy range. The data are determined by prehadronic and hadronic final state interactions. A consistent description of all these data can be obtained only if the prehadronic interaction strength grows linearly with time.

### 3 Hadronic Spectral Functions

In elementary reactions at lower energies and in ultrarelativistic heavy ion collisions the focus has always been on reconstructing the spectral function of hadrons in medium from the four-vector distributions of their decay products which are ultimately seen in the detector. Little attention has been paid to the fact that the observed invariant mass distribution is given by (in its simplest form) a product of production cross section  $\sigma_{\text{in}}$ , spectral function  $\mathcal{A}$  and decay branching ratio  $B_{\text{out}}$  which all three depend on the invariant mass  $\mu$  of the produced meson

$$\frac{d\sigma}{d\mu^2} \approx \sigma_{\text{in}}(\mu) \mathcal{A}(\mu) B_{\text{out}}(\mu) = \sigma_{\text{in}}(\mu) \frac{1}{\pi} \frac{\mu \Gamma_{\text{tot}}(\mu)}{(\mu^2 - m^2)^2 + \mu^2 \Gamma_{\text{tot}}^2(\mu)} B_{\text{out}}(\mu) . \quad (1)$$

The production cross section  $\sigma_{\text{in}}$  contains a phase-space factor that naturally favors the production of low-mass  $\omega$ 's. In addition, there is a sizeable final state interaction if one or both of the decay products are hadrons.

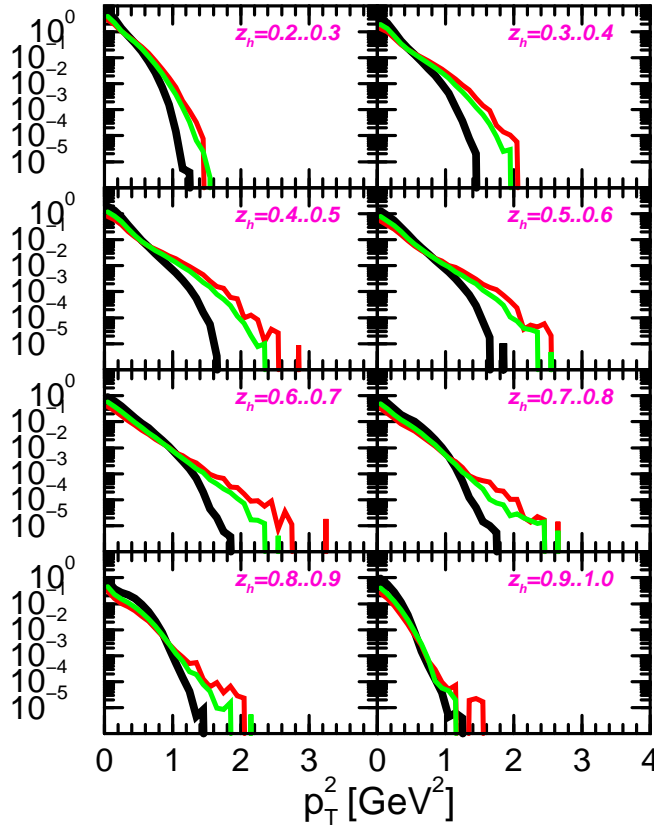


Figure 4: Transverse momentum spectra (arbitrary units) of  $\pi^+$  production on a  $Pb$  target for an electron energy of 5 GeV within the CLAS acceptance for different  $z_h$  bins. The solid line gives the distribution for a  $D$  target for comparison; the middle curve shows the results without and the top curve those with prehadronic interactions.

In ultrarelativistic heavy ion collisions the emission often happens from a thermalized state so that the mass-dependence of the production plays no role and the decay branching ratio is known if the experiment looks for dileptons, as the heavy ion experiments HADES, CERES and NA60 [12, 13, 14] do. These reactions have the advantage that high densities and/or temperatures are reached. They have the inherent disadvantage, however, that any experimental signal necessarily contains a time-integral over the whole reaction and thus states with different characteristics (preequilibrium, equilibrium at varying temperatures and densities, different states of matter (hadronic or QGP)). Any analysis of results from such reactions thus needs a description of the reaction dynamics that is as good as that of the static equilibrium in-medium properties of the hadron.

In contrast, in reactions with elementary probes on nuclei [15, 16, 17] most of the densities probed are below that of nuclear matter, but the nuclear state remains much more stationary and the medium is thus much better defined. However, in this case the primary production cross section may be strongly dependent on the mass of the produced hadron, in particular if the experiment is performed with bombarding energies close to threshold. This is, for example, the case for the CBELSA/TAPS experiment [16, 18] that exploits the reaction  $\gamma + A \rightarrow \pi^0 + \gamma + A^*$  to look for the in-medium spectral function of the  $\omega$  meson. This experiment uses incoming photons that cover an energy range from below the free  $\omega$  production threshold up to energies well above. In addition, in this experiment not only do the outgoing pions experience strong final state interactions, but also the branching ratio is strongly dependent on the invariant mass. This is easy to see since just under the  $\omega$  peak the decay channel  $\omega \rightarrow \rho\pi$  opens up so that the in-medium properties of the  $\rho$  meson do influence those of the  $\omega$  meson.

We have shown earlier that the GiBUU method describes the experimentally obtained spectral function very well [19] if a lowering of the  $\omega$  mass by 14 - 16% at saturation density is put in by hand<sup>1</sup>. GiBUU is a semiclassical event generator that has been developed to describe a wide range of nuclear reactions, from neutrino-induced over electroproduction reactions to heavy-ion reactions, all with the same physics input and the same code [5]. In this sense it is unique. Since the method has been extensively tested against data in all these different reactions we feel confident that we can now use it to explore the physics of the effects observed in the CBELSA/TAPS experiment. Fig. 5 shows the results of such a study. Immediately noticeable is that the calculated spectral function with all in-medium corrections included shows a broadening only on the low-mass side of the peak; the right side is nearly unaffected by the mass-shift and the broadening. The explanation for this observation is

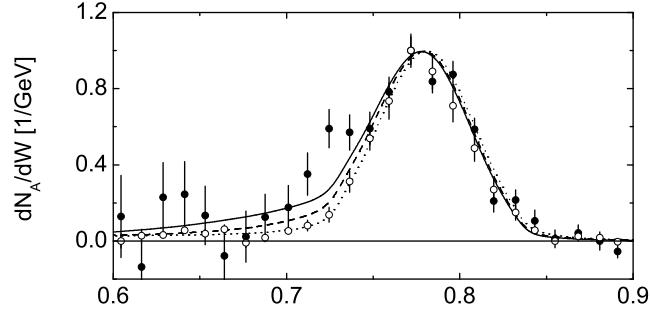


Figure 5: Comparison of calculated  $\omega$  spectral function as a function of the invariant mass (in GeV) in comparison to the data from [16] in the photon energy range 900 – 2200 MeV (open symbols: data on  $H$  target, solid: data on  $Nb$  target). The dotted curves contains only collisional broadening, the dashed curve contains the collisional broadening together with a downward mass shift of 8%, the solid curve finally contains broadening and a 16% downward mass shift (from [22]).

that the data have been taken in an energy-interval 900 – 2200 MeV that covers the free  $\omega$  production threshold at  $E_{\text{thresh}} = 1100$  MeV. Since the simulation contains an explicit mass shift in the spectral function this also shifts, correspondingly, the threshold for  $\omega$  production down. This downward shift of the threshold is the reason for the observed enhancement at lower masses.

In order to substantiate this explanation we show in Fig. 6 a comparison of the results of simulations for the reaction  $\gamma + {}^{40}\text{Ca} \rightarrow \pi^0 X$  in the photon energy intervals 900 – 1200 MeV (left), which covers the free  $\omega$  production threshold, and 1500 – 2000 GeV (right) which is clearly above the threshold.

Fig. 6 shows clearly that the low energy calculation (left) yields a very large surplus of strength on the low-mass side of the  $\omega$  peak, whereas at the higher energy nearly no enhancement can be seen. At the higher bombarding energy faster and faster  $\omega$  mesons are produced so that more and more of them will decay outside the nuclear target, with a free spectral function. Only with a very restrictive cut on  $\omega$  momenta, that enriches the in-medium decays, an effect could again be seen.

This strongly suggests that also the experimentally seen enhancement at the lower masses is due to a threshold effect. The production of  $\omega$  mesons in medium – with a lowered spectral function – is in the calculations described by first extracting the  $s$ -dependence of the matrix element from the free experimental cross section [23]

$$\sigma_{\gamma N \rightarrow \omega N}^{\text{exp}}(s) = \frac{1}{16\pi s |\mathbf{k}_{\text{cm}}|} \int_{m_\pi^2}^{(\sqrt{s}-m_N)^2} d\mu^2 |\mathcal{M}_{\gamma N \rightarrow \omega N}(s)|^2 \mathcal{A}_\omega(\mu, \rho=0) |\mathbf{q}_{\text{cm}}(\mu)| \quad (2)$$

under the assumption that the dependence of  $\mathcal{M}$  on the spectral function  $\mathcal{A}$  of the  $\omega$  meson in vacuum can be neglected. This gives the elementary cross section for  $\gamma + N \rightarrow \omega N$  shown in fig. 7. In a second

<sup>1</sup>Note that recent calculations of the  $\omega$  spectral function in medium give only a significantly smaller mass shift [20, 21].

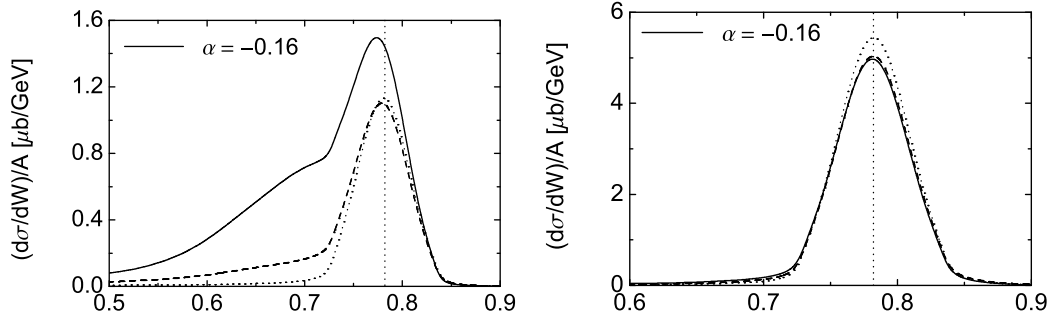


Figure 6: Invariant mass spectrum in the  $\pi^0\gamma$  channel from  $^{40}\text{Ca}$  in the photon energy range 900 - 1200 MeV (left) and 1500 - 2000 GeV (right). The results contain a folding with a mass resolution of 25 MeV and a  $1/E_\gamma$  weighting of a bremsstrahlung spectrum. The dotted lines give the vacuum spectral function, the dashed lines contain collisional broadening and the solid curves an attractive mass shift of 16% at saturation density (from [22]).

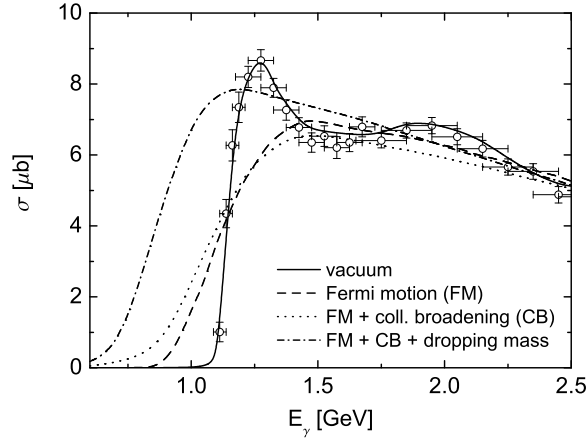


Figure 7: Total exclusive  $\omega$  production cross section. The curves including medium modifications are calculated at saturation density  $\rho_0$ . Data from [23] (from [22]).

step then, for use in the medium, the  $s$ -dependence of the matrix element is scaled (for details see [22]). After integrating over the Fermi motion and inserting an in-medium spectral function this gives the dash-dotted curve in Fig. 7. The difference between the solid (vacuum) and the dash-dotted (in-medium) curve is responsible for the effect seen in the CBELSA/TAPS experiment. If this treatment of the in-medium amplitude is sufficient for a realistic description of threshold effects will have to be more closely investigated now that the origin of the observed enhancement has been clarified.

## 4 Summary

Summarizing we emphasize again that any extraction of formation times and prehadronic interactions from nuclear attenuation data requires a state-of-the-art treatment of final state interactions that is as reliable as the QCD input. The same holds for experimental determinations of hadronic in-medium spectral functions where – besides the final state interactions – also the initial production process may play a significant role.

We gratefully acknowledge the discussions with and help of the whole GiBUU team: O. Buss, A. Larionov, T. Leitner, B. Steinmueller and J. Weil. This work has been supported by BMBF and DFG.

## References

- [1] K. Gallmeister and U. Mosel, Nucl. Phys. A (2008), in press [arXiv:nucl-th/0701064].
- [2] P. Muehlich and U. Mosel, Nucl. Phys. A **773**, 156 (2006) [arXiv:nucl-th/0602054].
- [3] T. Falter, W. Cassing, K. Gallmeister and U. Mosel, Phys. Rev. C **70** (2004) 054609 [arXiv:nucl-th/0406023].
- [4] K. Gallmeister and T. Falter, Phys. Lett. B **630** (2005) 40 [arXiv:nucl-th/0502015].
- [5] <http://gibuu.physik.uni-giessen.de/GiBUU/>
- [6] Y. Dokshitzer, V. Khoze, A. Mueller and S. Troyan, *Basics of perturbative QCD*, Editions Frontiers (1991)
- [7] B. Z. Kopeliovich and B. G. Zakharov, Phys. Rev. D **44** (1991) 3466.
- [8] A. Airapetian *et al.* [HERMES Collaboration], Nucl. Phys. B **780** (2007) 1 [arXiv:0704.3270 [hep-ex]].
- [9] G. R. Farrar, H. Liu, L. L. Frankfurt and M. I. Strikman, Phys. Rev. Lett. **61**, 686 (1988).
- [10] B. Clasie *et al.*, arXiv:0707.1481 [nucl-ex].
- [11] M. Kaskulov, K. Gallmeister and U. Mosel, to be published
- [12] I. Frohlich *et al.* [HADES Collaboration], Eur. Phys. J. A **31** (2007) 831 [arXiv:nucl-ex/0610048].
- [13] D. Adamova *et al.*, arXiv:nucl-ex/0611022.
- [14] S. Damjanovic *et al.* [NA60 Collaboration], Nucl. Phys. A **783** (2007) 327 [arXiv:nucl-ex/0701015].
- [15] R. Nasseripour, M. H. Wood, C. Djalali, D. P. Weygand, C. Tur, U. Mosel, P. Muehlich, CLAS Collaboration, Phys. Rev. Lett. (2007) in press [arxiv.org/abs/0707.2324v3].
- [16] D. Trnka *et al.* [CBELSA/TAPS Collaboration], Phys. Rev. Lett. **94** (2005) 192303 [arXiv:nucl-ex/0504010].
- [17] S. Yokkaichi *et al.* [KEK-PS325 Collaboration], Int. J. Mod. Phys. A **22**, 397 (2007).
- [18] V. Metag, these proceedings, arXiv:0711.4709 [nucl-ex].
- [19] P. Muehlich, T. Falter and U. Mosel, Eur. Phys. J. A **20** (2004) 499 [arXiv:nucl-th/0310067].
- [20] P. Muehlich, V. Shklyar, S. Leupold, U. Mosel and M. Post, Nucl. Phys. A **780** (2006) 187 [arXiv:nucl-th/0607061].
- [21] M. F. M. Lutz, G. Wolf and B. Friman, Nucl. Phys. A **706** (2002) 431 [Erratum-ibid. A **765** (2006) 431] [arXiv:nucl-th/0112052].
- [22] P. Muehlich, PhD thesis, University of Giessen, 2007 [<http://theorie.physik.uni-giessen.de/documents/dissertation>]
- [23] J. Barth *et al.*, Eur. Phys. J. A **18** (2003) 117.